Physica C 469 (2009) 1536–1540

Contents lists available at ScienceDirect

Physica C

journal homepage: www.elsevier.com/locate/physc

Microstructure and superconducting properties comparison of bronze and internal tin process Nb_3Sn strands for ITER

P.X. Zhang [a,b,*], Y. Feng [a,b], X.H. Liu [b], C.G. Li [a], K. Zhang [b], X.D. Tang [a,b], Y. Wu [c]

[a] Northwest Institute for Non-ferrous Metal Research, Xi'an, Shaanxi 710016, PR China
[b] Western Superconducting Technologies Co. Ltd., Xi'an, Shaanxi 710016, PR China
[c] Institute of Plasma Physics, Chinese Academy of Sciences, Hefei 230031, PR China

ARTICLE INFO

Article history:
Available online 12 June 2009

PACS:
74.70.Ad
74.60.Jg
75.60.Ej

Keywords:
Nb_3Sn
Internal Sn and bronze process
Microstructure
Superconducting properties

ABSTRACT

The long multifilamentary Nb_3Sn strands for international thermonuclear experimental reactor (ITER) have been successfully fabricated by bronze and internal Sn process, respectively. Adopted in this work, the bronze process Nb_3Sn strand with a Cu/non-Cu area ratio of 1:1.09 and the internal tin process strand with a Cu/non-Cu area ratio of 1:1.15 were designed. The microstructure details of two kinds of strands before and after heat treatment have been investigated by scanning electron microscope (SEM) and energy dispersive X-ray analysis (EDX). The non-Cu J_c (12 T, 4.2 K) value of 752 A/mm^2 for bronze process strand and 1185 A/mm^2 for internal tin process strand have been obtained. The influence of microstructure on transport property of strands has been discussed.

1. Introduction

Ever since its discovery, Nb_3Sn superconductor has received substantial attention due to its possibility to carry very large current densities far beyond the limits of the commonly used NbTi. Recently Nb_3Sn has been intensively studied due to its high upper critical field (H_{c2}) [1], which is the best candidate for fabrication of high-field magnets and toroidal field coils of international thermonuclear experimental reactor (ITER) up to now. Several fabrication methods, such as bronze process [2], internal Sn process [3], powder in tube (PIT) process [4] and modified jelly roll process (MJR) [5], etc., have been developed for fabrication of high performance superconducting Nb_3Sn wires. Only the bronze process and internal tin process, however, have become dominant due to their commercial potentials. In the case of the bronze process, the maximum volume fraction of Nb_3Sn phase is limited by the bronzing process between Cu and Sn, where the Sn content in the bronze matrix is not larger than 13.5 wt%. In order to overcome insufficiency of Sn source in bronze route the internal tin concept was proposed to allow high volume fractions of Nb_3Sn resulting in a high-J_c value. But for internal tin process, the percentage of Nb_3Sn layers has to be controlled in an appropriate scope in order to prevent filament coupling to decrease the hysteresis loss.

ITER project has already given a series of technical and physical specifications to Nb_3Sn strand prepared by internal tin and bronze route. A lot of research groups and companies have been making efforts to reach these required specifications [6–8]. And many different fabrications and results have been reported [8–10]. Three key problems have to be solved in the fabrication of Nb_3Sn strands. Firstly, the unit length of strands must exceed 1.5 km, where any filament break should be avoided during strand processing. Secondly, the J_{cn} (non-Cu area J_c) could be increased, whereas the hysteresis loss should be lowered. Thirdly, the filaments of Nb_3Sn strands should be uniform (about 3–4 μm) in order to get an n-value larger than 20. The effects of "sausaging" of filaments along the length direction of strands, which is caused by different deformation behavior of filaments, should be eliminated.

In this work, we report the fabrication of multifilamentary Nb_3Sn strands by internal tin and bronze process and investigate their microstructure and superconducting properties.

2. Experimental details

For the fabrication of bronze Nb_3Sn strands in this work, 37 pieces of NbTa alloy rods are inserted in a high 15 wt% Sn bronze matrix with Ti doping, which is surrounded by stabilization Cu.

* Corresponding author. Address: Northwest Institute for Non-ferrous Metal Research, Xi'an, Shaanxi 710016, PR China. Tel.: +86 29 862310769; fax: +86 29 86224487.
E-mail address: pxzhang@c-nin.com (P.X. Zhang).

0921-4534/$ - see front matter © 2009 Elsevier B.V. All rights reserved.
doi:10.1016/j.physc.2009.05.236

Then the complete billet with weight of about 50 kg, which consist 313 subfilaments, is drawn to diameter of 0.82 mm with 11,581 Nb7.5Ta filaments. The bronze area represents the Sn source and is surrounded by Ta barrier that prohibits the Sn from diffusing into the high purity stabilization Cu. Our internal tin process strand comprises a Cu stabilizer, a Cu/Ta barrier and 19 subfilaments, which consist of about 324 Nb filaments in a Cu matrix surrounding a Sn–Ti core. The weight of billets with 19 subfilaments could reach 50 kg and the unit length of final strands with a strand diameter of 0.79 mm could be 3000–5000 m. The cross-section view of as-drawn internal tin and bronze Nb_3Sn stands is shown in Fig. 1 and the typical parameter of strands are shown in Table 1.

For getting the transport properties the internal tin and bronze process Nb_3Sn strand about 1 m was wound on a mandrel according the standard measurement method of superconducting critical current. Based on consideration of thermal expansion coefficients Ti_6Al_4V was selected as mandrel materials which were coated with graphite to prevent conglutination. The heat treatment time for wires was carried according in vacuum the standard process for ITER specification (shown in Fig. 2). The critical current of wires was measured utilizing the 4-probe method at magnetic fields at 4.2 K. I_c was determined by a criterion of 0.1 μV/cm. The distance of voltage contacts was 50 cm. The n-value was calculated as the slope of the log V–log I plot between 0.1 and 1 μV/cm using a least mean square fit. The microstructure of strand was investigated by a JEOL JSM-5410 scanning electron microscope (SEM) and energy dispersive X-ray analysis (EDX).

3. Results and discussion

The overall cross-section of as-drawn bronze process strands with 313 subfilaments and internal tin process strand with 19 subfilaments are shown in Fig. 1. The bronze process strand with 313 subfilaments has 11,581 NbTa filaments with diameter of about 3 μm (Fig. 1a). The internal tin process strand with 19 subfilaments has 6156 Nb filaments and the filament size of strands is about 3–4 μm (Fig. 1b). The Ta barrier thickness is about 6–10 μm for the two strands. By SEM we have observed no leak in Ta barrier layer. To obtain high-J_c Nb_3Sn stands, the processing parameters were optimized and series of experiments were performed. As a result, the internal tin process Nb_3Sn single strand adopted in this work with a Cu/non-Cu area ratio of 1:1.15 and bronze process strand with a Cu/non-Cu area ratio of 1:1.09 are designed as shown in Table 1.

After cold working of strands the heat treatment is a key process for obtaining high-J_c Nb_3Sn multifilamentary strand. It directly affects the volume fraction of Nb_3Sn phase and also the quality of Nb_3Sn phase itself. In the case of bronze process, heat treatment temperature is just between 650 °C and 750 °C to form the A15 Nb_3Sn phase by solid state diffusion. In the case of internal Sn process, however, the heat treatments are designed to realize two functions: (1) to form Sn–Cu alloy at low temperature and (2) to form A15 phase at high temperature. The heat treatment schedule applied was recommended by the ITER specification as shown in Fig. 2.

Fig. 3 shows the SEM images of various regions of bronze process strands after heat treatment. It is clear that no un-reacted Nb can be found even in the parts close to the Ta barrier, as shown Fig. 3a, which indicate that the supply and diffusion of Sn source is homogenous though the whole strand cross-section. For a selected filament in the central parts, we have in detailed investigated the grain morphology and composition by SEM and EDS. Typical results are shown in Fig. 3b and c. Fig. 3b shows a magnification of the filament region at the edge within strand in which the A15 phase is visible as light gray area distinguished and some voids can be found also in bronze matrix. Fig. 3c depicts a fracture surface of a filament, which shows that mainly columnar grains are formed with average grain size of about 80 nm. EDS analysis has

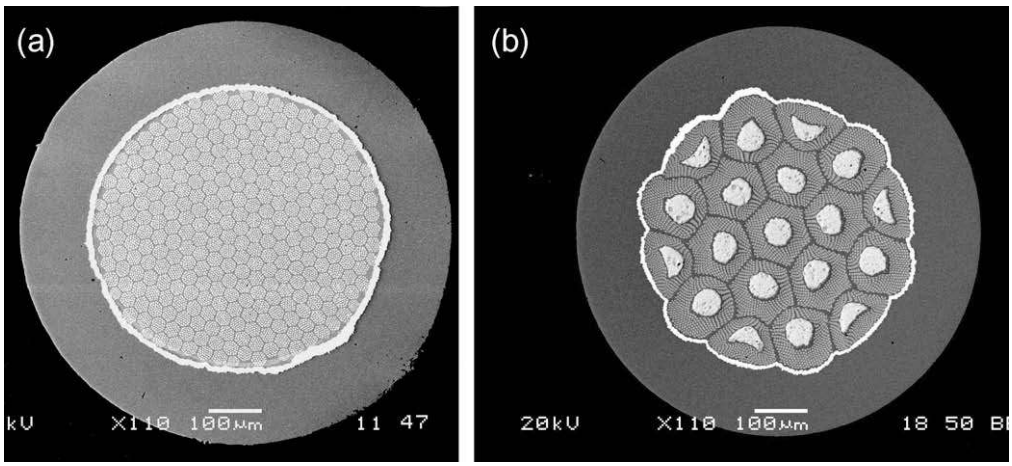

Fig. 1. The SEM cross-section of as-drawn Nb_3Sn strands. (a) Φ0.79 mm bronze process strand (37 × 313 filaments) and (b) Φ0.81 mm internal tin process strand (19 × 330 filaments).

Table 1
The parameters for Nb_3Sn strands.

	Bronze process strand	Internal tin process strand
Diameter (mm)	0.82	0.79
Filaments	37 × 313 NbTa filaments	19 × 324 Nb filaments
Filament size	~3 μm	3–4 μm
Ta layer	8–10 μm	6–10 μm
Ratio of Cu and non-Cu area	1.09	1.15
$J_{c\ non\text{-}cu}$ (A/mm^2)	752	1185

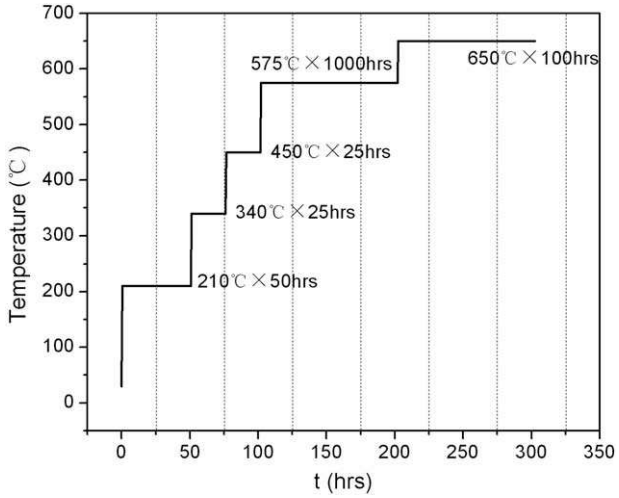

Fig. 2. Process flow diagram of heat treatment for all strands.

shown that the atomic ration Nb/Sn in the central parts of strands is very close to the chemical stoichiometry of 3:1 as indicated in Fig. 3d. This result indicates that for our sample the Sn diffusion and the growth process of A15 grains are improved by using high Sn content bronze and employing fine fabrication process. However, the effects of the addition of Ti in the Cu–Sn–Ti tube and Ta in the Nb–Ta bars on the Sn diffusion and on the growth of Nb_3Sn phase should be investigated deeply in the future [11].

Fig. 4 shows the SEM images of various regions of internal tin process strands after heat treatment. For the strands annealed at 650 °C for 100 h, we could not detected the un-reacted Nb in the central parts of strands, as shown in Fig. 4a and b. In the parts close to the Ta barrier, un-reacted Nb areas were not fully eliminated. Therefore it is reasonable to believe that the supply and diffusion of Sn source is in fact not homogenous though the whole strand cross-section. For a selected filament in the central parts, where the reaction of formation of Nb_3Sn phase is finished, we have in detailed investigated the grain morphology and composition by SEM and EDS. Typical results are shown in Fig. 4c and d. We have found that the grain morphology differs at the center and the edge within one filament. Nb_3Sn grains are almost equiaxed grains at the edge, whereas columnar grains exist in the core of the filaments (see Fig. 4c). Average grain diameters are 96 nm. EDS analysis has shown that although the atomic ration Nb/Sn in the central parts of strands is very close to the chemical stoichiometry of 3:1, the region of columnar grains in the core of filaments is Nb-rich as indicated in Fig. 4d. This is related to the Sn diffusion and the growth process of Nb_3Sn grains. As we studied before, the existence of columnar Nb_3Sn grains will affect the quality of Nb_3Sn layers, because the deviation from ideal chemical stoichiometry strongly degenerates the superconducting property of Nb_3Sn layer itself [12]. The exact control of Sn diffusion and Nb_3Sn grain growth is to be solved in the future. Moreover, the effects of the addition

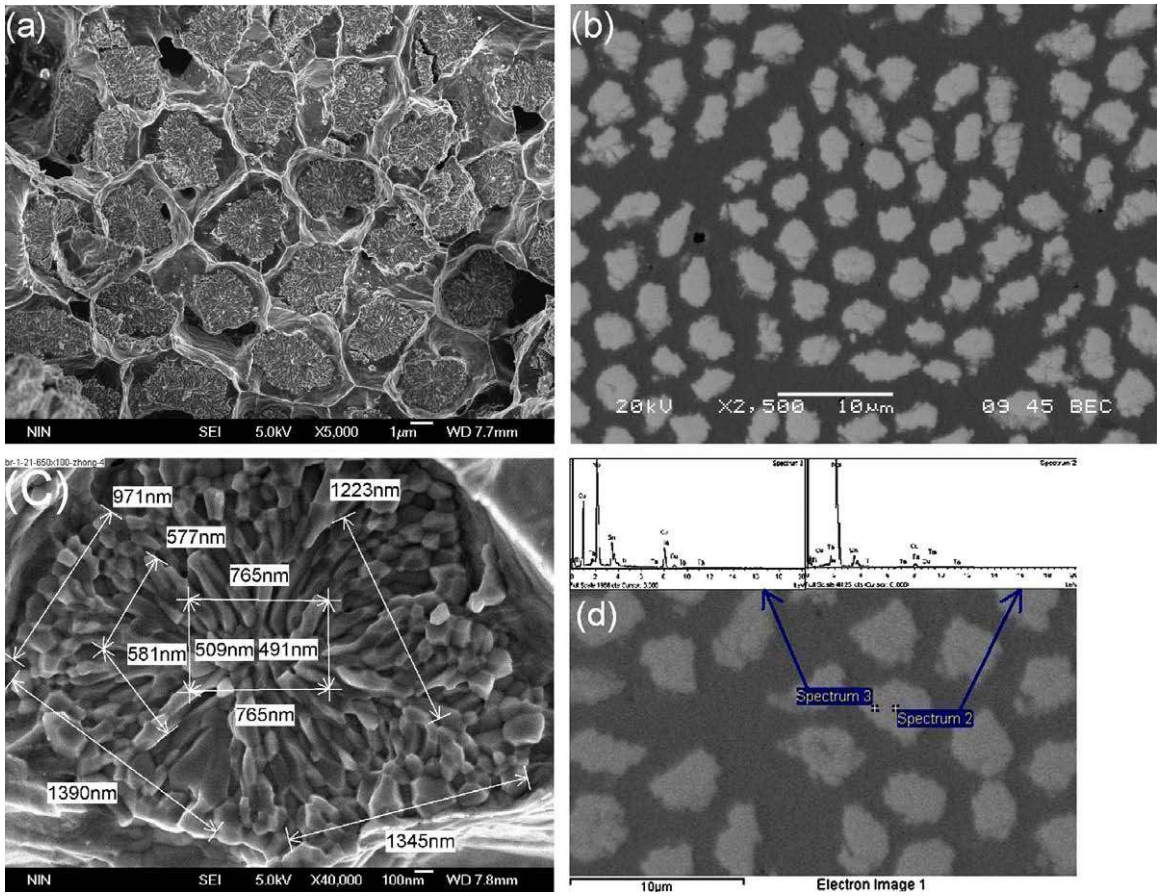

Fig. 3. SEM images and EDS analysis after heat treatment for bronze process Nb_3Sn strands. (a) SEM image for strands after heat treatment of 650 °C/100 h; (b) SEM image of the central parts of strands after heat treatment of 650 °C/100 h; (c) grain morphology of Nb_3Sn layers after heat treatment of 650 °C/100 h; and (d) EDS analysis of Nb_3Sn layers.

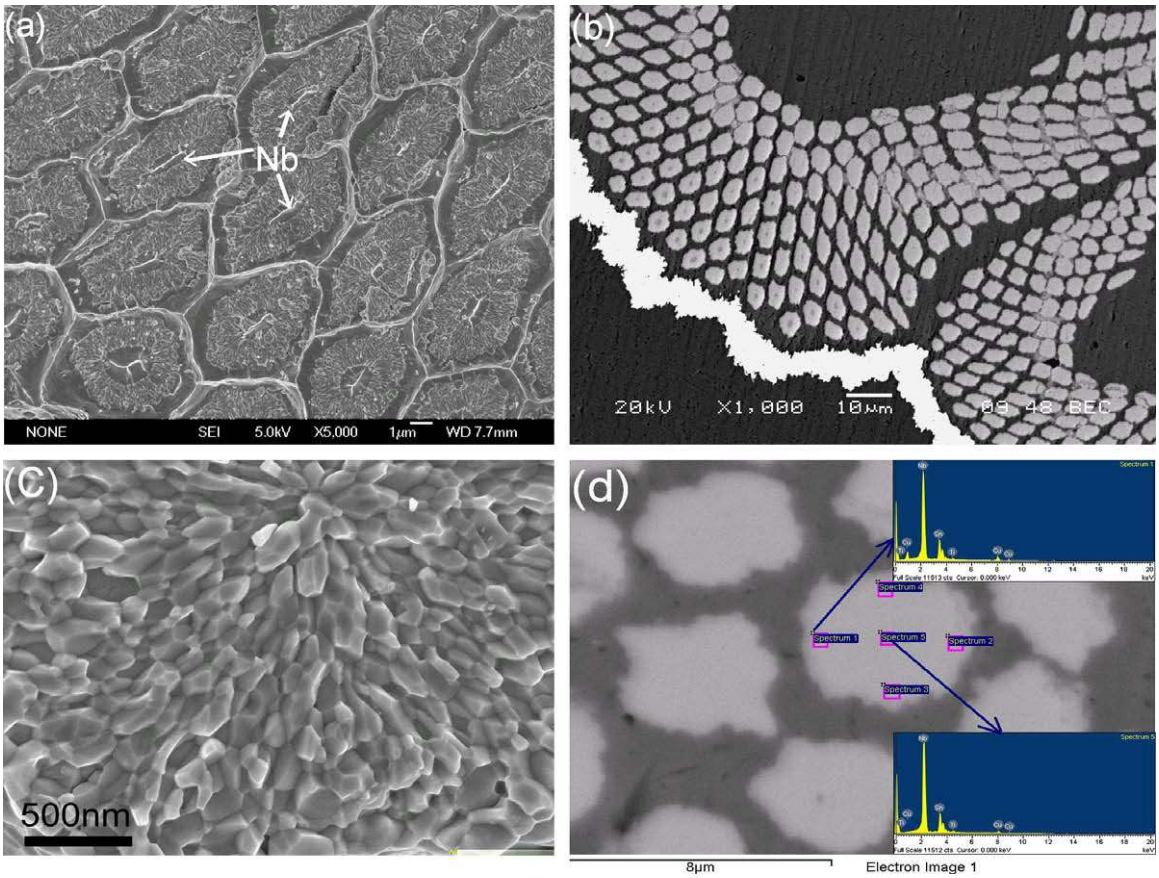

Fig. 4. SEM images and EDS analysis after heat treatment for internal process Nb_3Sn strands. (a) SEM image for strands after heat treatment of 650 °C/100 h; (b) SEM image of the central parts of strands after heat treatment of 650 °C/100 h; (c) grain morphology of Nb_3Sn layers after heat treatment of 650 °C/100 h; and (d) EDS analysis of Nb_3Sn layers.

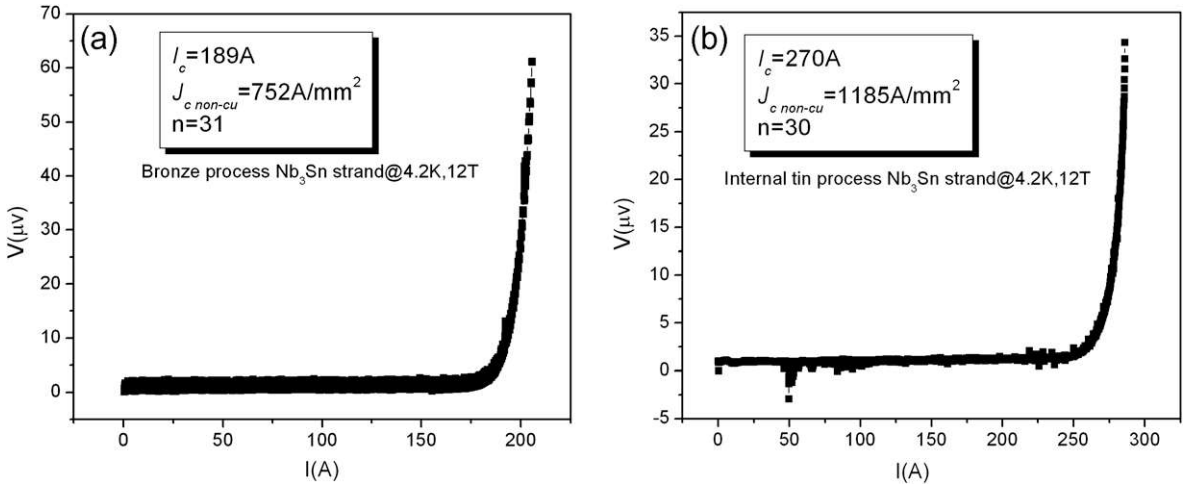

Fig. 5. The transport properties of Nb_3Sn strands. (a) *V–I* curves measured at 4.2 K, 12 T for bronze process strand and (b) *V–I* curves measured at 4.2 K, 12 T for internal tin process strand.

of Ti in the Sn–Ti core on the Sn diffusion and on the growth of Nb_3Sn should be quantitatively evaluated.

Fig. 5 shows measurement results of the transport property for typical samples prepared by bronze and internal tin process. According to the standard method of I_c measurement we have given the *V–I* curves at 4.2 K in 12 T. The non-Cu critical current density J_{cn} of bronze process and internal tin process Nb_3Sn strand could reach 1185 A/mm^2 and 752 A/mm^2 at 4.2 K in 12 T, respectively. Since the grain boundary is believed as pinning centers in Nb_3Sn superconductors [13,14], grain refining is useful to increase

J_{cn}. J_{cn} depends on the volume percentage of stoichiometric Nb_3Sn layers in the whole strand and also on the quality of superconducting Nb_3Sn layers.

The n-value derived from V–I curves at the superconducting-to-normal state transition can reflect the abruptness of the transition. By the n-value the quality of strands as a whole can be evaluated very simply. For multifilamentary strands the n-value becomes to be dependent on the distribution of the properties of filaments. For our bronze and internal tin process Nb_3Sn strands the n-value from $V \propto I^n$ at 4.2 K and 12 T reaches 31 and 30, respectively, which meet the specification of ITER. The increase of the n-value actually depends on the improvement of fabrications for higher homogeneity of strands. Both the high-J_c and the high n-value should be simultaneously considered for ITER type strands. But it is clear that for internal tin process Nb_3Sn strand the percentage of Nb_3Sn layers has to be controlled in an appropriate range in order to prevent the coupling among filaments to decrease the hysteresis loss.

4. Summary

By bronze and internal tin process respectively, long multifilamentary Nb_3Sn strands for ITER with a unit length larger than 2 km have been successfully fabricated. The microstructure analysis and critical current measurement results have indicated that the conductor design, fabrication and the heat treatment of Nb_3Sn strands affect the volume fractions of Nb_3Sn layers, Nb_3Sn stoichiometry and the size of grains. The non-Cu J_c (12 T, 4.2 K) value reaches 752 A/mm^2 for bronze process strand and 1185 A/mm^2 for internal tin process strand. The main specifications have reached the demand by ITER.

Acknowledgement

This work was supported by the National 973 Program of China (Contract No. 2006CB601004).

References

[1] T. Ando, J. Cryogen. Soc. Jpn. 39 (2004) 38.
[2] A.R. Kaufmann, J.J. Picett, Bull. Am. Phys. Soc. 15 (1970) 838.
[3] Y. Hashimoto, K. Yoshizaki, M. Tanaka, in: Proc. 5th ICEC, 1974, p. 332.
[4] J.D. Elen, C.A.M. van Beijnen, C.A.M. van der Klein, IEEE Trans. Magnet. MAG-13 (1977) 470.
[5] W.K. McDonald, C.W. Curtis, R.M. Scanlan, D.C. Larbalestier, K. Marken, D.B. Smathers, IEEE Trans. Magnet. MAG-19 (1983) 1124.
[6] ITER Web Page (Online), <http://www.iter.org>.
[7] R.M. Scanlan, IEEE Trans. Appl. Supercond. 11 (2001) 2150.
[8] K. Tachikawa, J. Cryogen. Soc. Jpn. 39 (2004) 377.
[9] R.M. Scanlan, D.R. Dietderich, S.A. Gourlay, Adv. Cryogen. Mater. 50 (2004) 349.
[10] A.F. Lietzke, P. Ferracin, S.A. Gourlay, S. Mattafirri, M. Nyman, G. Sabbi, G. Ambrosio, S. Feher, B. Bordini, IEEE Trans. Appl. Supercond. 14 (2004) 283.
[11] K. Zaitsu, H. Kato, T. Miyazaki, T. Hase, M. Hamada, J. Cryogen. Soc. Jpn. 43 (2008) 15.
[12] P.X. Zhang, L. Zhou, X.D. Tang, C.G. Li, Y. Wu, K. Li, G. Yan, M. Yang, Y. Feng, X.H. Liu, P.D. Weng, Y.F. Lu, Physica C 445–448 (2006) 819.
[13] R.M. Scanlan, W.A. Fietz, E.F. Koch, J. Appl. Phys. 46 (1975) 2244.
[14] S. Ochiai, L. Osamura, Acta Metall. 34 (1986) 2425.